Homothorax Switches Function of *Drosophila* Photoreceptors from Color to Polarized Light Sensors

Mathias F. Wernet,[1] Thomas Labhart,[2]
Franziska Baumann,[2] Esteban O. Mazzoni,[1]
Franck Pichaud,[1,3] and Claude Desplan[1,*]
[1]New York University
Department of Biology
100 Washington Square East
New York, New York 10003
[2]Universität Zürich
Zoologisches Institut
Winterthurerstr. 190
CH-8057 Zürich
Switzerland

Summary

Different classes of photoreceptors (PRs) allow animals to perceive various types of visual information. In the *Drosophila* eye, the outer PRs of each ommatidium are involved in motion detection while the inner PRs mediate color vision. In addition, flies use a specialized class of inner PRs in the "dorsal rim area" of the eye (DRA) to detect the e-vector of polarized light, allowing them to exploit skylight polarization for orientation. We show that *homothorax* is both necessary and sufficient for inner PRs to adopt the polarization-sensitive DRA fate instead of the color-sensitive default state. Homothorax increases rhabdomere size and uncouples R7-R8 communication to allow both cells to express the same opsin rather than different ones as required for color vision. Homothorax expression is induced by the iroquois complex and the wingless (wg) pathway. However, crucial wg pathway components are not required, suggesting that additional signals are involved.

Introduction

Animals have developed many different light-sensing structures as eyes are optimized to the animal's environment, allowing the processing of maximum amounts of information by perceiving different parameters of the visual world. Photoreceptors (PRs) are sensitive to light intensity, spectral composition, and the state of polarization of a stimulus. The visual system disentangles and processes the information provided by the receptors such that animals exhibit form vision, color vision, and polarization vision.

The adult *Drosophila* eye is composed of ~800 ommatidia, each containing eight PRs, as well as cone, pigment, and bristle cells (for review see Wolff, 1993). In each ommatidium, a group of six "outer PRs" (R1 through R6) are equipped with light gathering structures (rhabdomeres) that span the entire retina. These PRs all express the same blue/green sensitive rhodopsin (Rh1, Zuker et al.,
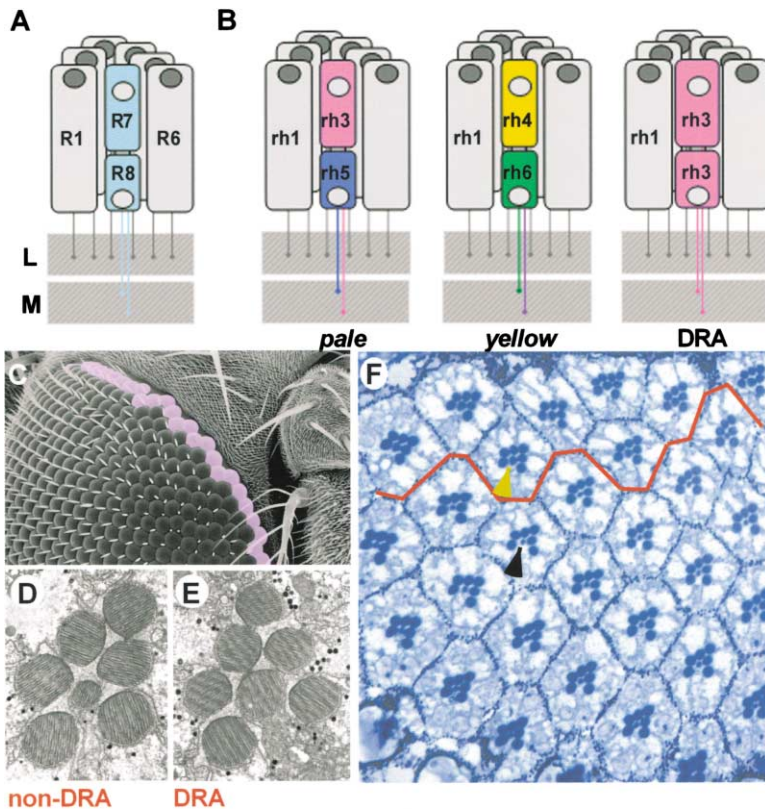
1985). They project to the first optic ganglion, the lamina, where visual information relevant for form vision and motion detection starts to be processed (Hardie, 1985). The inner PRs have R7 sitting on top of R8, dividing the adult retina into two concentric layers (Figure 1A). R7 and R8 express only one opsin gene out of a repertoire of four inner PR opsins that exhibit different spectral sensitivities. They project to the second optic ganglion, the medulla, with R7 terminating in a deeper layer than R8.

Based on their morphology and the type of opsin expressed in their inner PRs, the ommatidia can be grouped into three categories (Figure 1B). The "pale" (p) and "yellow" (y) ommatidia are stochastically distributed throughout the main part of the retina (p: ~30%/y: ~70%; Franceschini et al., 1981; Kirschfeld and Franceschini, 1977). Compared to the outer PRs surrounding them, the rhabdomere diameter of inner PRs in these two subtypes is significantly reduced (Figure 1D; Wolff, 1993). Pairing of the opsins expressed in these R7 and R8 cells is tightly regulated; pale ommatidia express the UV-sensitive Rh3 in R7 and the blue-sensitive Rh5 in R8, while yellow ommatidia express Rh4 (UV-sensitive) in R7 and Rh6 (green-sensitive) in R8 (Chou et al., 1996; Papatsenko et al., 1997; Huber et al., 1997). These two classes of ommatidia are thought to be crucial for the fly's ability to discriminate amongst various colors (Kirschfeld and Franceschini, 1968) and we will refer to them as "color-sensitive." A third class comprises one, or sometimes two rows of ommatidia at the dorsal margin of the eye, the dorsal rim area (DRA). These ommatidia appear to serve as detectors for the oscillation plane (e-vector orientation) of linearly polarized light (Wada, 1974; Hardie, 1984) and we will refer to them as "polarization-sensitive." On its way through the atmosphere, unpolarized sunlight is scattered by air molecules and, as a result, skylight is partly polarized. At any point of the sky, a particular e-vector orientation dominates depending on the position of the sun (see Wehner, 1994; Labhart and Meyer, 2002) producing a polarization pattern that forms the basis for a polarization compass demonstrated for many insect species (Wehner, 1994; Labhart and Meyer, 1999). Polarization sensitivity was demonstrated in flies by using a behavioral approach (von Philipsborn and Labhart, 1990; Wolf et al., 1980) and DRAs have been described morphologically in a multitude of insect species (Labhart and Meyer, 1999). Hence, *Drosophila* and many other insects should be able to detect skylight polarization and use it as a reference for orientation.

In the DRA of *Drosophila*, the inner PRs (R7 and R8) have uniquely adapted their configuration and morphology to polarized light detection. (1) As shown in larger fly species, the inner PRs are strongly polarization-sensitive, which is due to strict alignment of the microvilli that form the rhabdomere. In all other PRs, polarization sensitivity is weak because the microvilli are misaligned by rhabdomere twisting (Hardie, 1984; Wunderer and Smola, 1982). (2) The diameter of both inner PR rhabdomeres is significantly enlarged (Figures 1E–1F and

Figure 1. Ommatidia in the Dorsal Rim Area

(A) Ommatidial subtypes in the *Drosophila* eye: each ommatidium contains 8 photoreceptor cells (PRs: R1 to R8). Rhabdomeres of outer PRs (R1 to R6) span the whole retina and their axons project to the lamina (L) part of the optic lobe. Inner PRs (R7 and R8) are located on top of each other and both project axons to the medulla (M).

(B) Ommatidia fall into three categories based on rhabdomere morphology and opsin expression. Inner PRs of pale and yellow ommatidia produce rhabdomeres of small diameter and can be distinguished by their characteristic opsin expression (p: rh3/*rh5* versus y: *rh4/rh6*). Specialized ommatidia are found exclusively in the dorsal rim area (DRA) of the adult eye, manifesting large inner PR rhabdomere diameters and *rh3* expression in both R7 and R8.

(C) Scanning electron micrograph showing the frontodorsal region of the eye. One and sometimes two rows of ommatidia at the dorsal eye rim row (pink) are specialized for polarization vision.

(D–E) Electron micrographs of cross-sections through ommatidia located outside the DRA (D) and within the DRA (E). The central rhabdomeres of DRA ommatidia are markedly enlarged.

(C–E) are used with permission from Labhart and Meyer, 1999.

(F) Light micrograph of an epon thin section through the dorsalmost part of the eye. There is a clear boundary (red line) between DRA ommatidia with wide inner PR rhabdomeres (yellow arrow) and non-DRA ommatidia with narrow rhabdomeres (black arrow).

R, retina; L, lamina; M, medulla.

Wada, 1974), enhancing sensitivity. (3) The microvilli of R7 and R8 are oriented orthogonally to each other (Wunderer and Smola, 1982) indicating that these cells are tuned to e-vector orientations that differ by 90° (Hardie, 1984). R7 and R8 project to the medulla and are believed to interact antagonistically via polarization-sensitive interneurons to enhance polarization sensitivity, a processing mechanism demonstrated for other insects (Labhart, 1988, 2000; Rossel and Wehner, 1986; for review, Labhart and Meyer, 2002). (4) Both R7 and R8 express the UV-sensitive opsin Rh3 (Fortini and Rubin, 1990, 1991). Thus, the polarization compass is monochromatic and hence color-blind, so that any ambiguity between information about color and polarization is eliminated.

During third instar larval life, *Drosophila* PRs are recruited from an undifferentiated pool of progenitor cells in a wave of differentiation called the "morphogenetic furrow" (MF) that sweeps through the imaginal disc starting at the posterior edge. In undifferentiated cells anterior to the furrow, the eye imaginal disc is subdivided into dorsal and ventral compartments (McNeill et al., 1997) whose interface will later become the equator of the eye. The dorsal selector genes *araucan* (*ara*), *caupolican* (*caup*), and *mirror* (*mirr*) encode homologous homeodomain transcription factors forming the Iroquois complex (*IRO-C*). During early larval stages prior to the MF, these genes become specifically expressed in the territory that will give rise to the dorsal eye and head

capsule (for review, Cavodeassi et al., 2001). The *IRO-C* complex is activated very early during eye development by the diffusible morphogen *wingless* (*wg*). At later stages, *wg* expression then becomes restricted to dorsal and ventral poles of the imaginal disc (Treisman and Rubin, 1995). IRO-C is necessary for specification of characteristic dorsal structures like head capsule, dorsal bristles, and ocelli as well as the establishment of the dorsoventral pattern organizer (that is later associated with the "equator" (Cavodeassi et al., 2001; Pichaud and Casares, 2000).

Cells posterior to the MF differentiate over several days in a process, which can conceptually be subdivided into two consecutive steps. First, during late larval life, the ommatidia are continuously recruited into evenly spaced clusters (Brennan and Moses, 2000); the PR axons immediately project to their respective optic lobes and the ommatidial clusters rotate. In a second step, during pupation, the retina undergoes massive morphogenesis leading to its terminal differentiation. This process includes the formation of PR rhabdomeres and the expression of visual pigments (Wolff, 1993). Recently, we have shown that the *spalt* gene complex is necessary for one of the first PR maturation steps: specification of both R7 and R8 as inner rather than outer PRs (Mollereau et al., 2001). *prospero* is then required in R7 to distinguish its fate from an R8-like ground state, while *senseless* specifies final R8 differentiation (Cook et al., 2003).

Here, we show that the homeodomain transcription factor Homothorax plays a critical role for DRA development: *hth* is expressed specifically in maturing inner PRs of the DRA and maintained through adulthood. We demonstrate that *hth* is both necessary and sufficient for the development of these polarization-sensitive PRs; loss of *hth* results in the transformation of the DRA into color-sensitive ommatidia, and misexpression of *hth* forces color-sensitive inner PRs to acquire the typical features of polarization-sensitive DRA cells. Furthermore, we show that the dorsal selector genes of the *IRO-C* complex are sufficient to induce *hth* expression DRA as well as features in the "ventral rim area" when misexpressed there. Finally, we show that activating the *wg* pathway is sufficient to induce DRA development throughout the dorsal eye. However, none of the key mediators of the Wg pathway seems to be required for DRA formation. Additional signals might induce the DRA in parallel or downstream of Wg.

Results

Inner Photoreceptors in the DRA Express Homothorax

To identify genes controlling late PR maturation events, we performed a GAL4 enhancer trap screen (Brand and Perrimon, 1993) in adult PRs using GFP as a reporter gene (Mollereau et al., 2000). One of the insertions was expressed in a single row of ommatidia along the dorsal head cuticle, as detected by neutralizing the cornea using water immersion microscopy in living flies (Franceschini and Kirschfeld, 1971; Pichaud and Desplan, 2001; Figure 2A). In some locations, two (but never more) positive rows of ommatidia were observed (data not shown). We visualized the projections of the GAL4-positive cells to the optic lobe with UAS-lacZ; all marked axons terminated in the dorsalmost part of the medulla with projections to both R7 and R8 layers (Figure 2B), indicating that GAL4 was expressed exclusively by inner PRs in the DRA. We determined that the insertion was in the second intron of *homothorax* (*hth*) (Rieckhof et al., 1997). To verify that the observed GAL4 expression pattern in developing DRA inner PRs was indeed that of endogenous Hth protein, pupal retinas (~48 hr after puparium formation, APF) were stained with an antibody against Hth (Figures 2C and 2D). Hth expression was always detected in one, at most two rows of ommatidia and only at the dorsal rim of the pupal retina (Figure 2C). The majority of positive ommatidia expressed Hth in two cells per cluster, which were identified as R7 and R8 because of their stereotypical positioning as compared to the landmark *svp*-lacZ (Wolff, 1993). Ommatidia with only one Hth expressing cell could also rarely be observed without showing any obvious preference toward R7 or R8. Hth expression was maintained throughout adulthood (Figure 2D) and was coexpressed with the R7 UV-opsin Rh3, which is the only opsin expressed by both inner PRs of the DRA (Fortini and Rubin, 1990). Rh3-expressing R7 cells outside of the DRA were always negative for Hth. Therefore, Hth is a highly specific marker for the polarization-sensitive inner PRs of the DRA.

Development of the DRA

We characterized the time-course of Hth expression in PRs to better understand the possible signaling pathways involved in DRA development. Hth is never detected in developing PRs of third instar eye imaginal discs but it is expressed in undifferentiated cells anterior to the MF as well as in pigment progenitor cells (Pichaud and Casares, 2000; Bessa et al., 2002; Figure 3A). This latter expression disappeared after 50% pupation. Early in pupation (between 5%–10%), Hth became expressed in two PR cells per cluster (rarely, only one positive cell was observed) in one or two of the dorsalmost ommatidial rows and remained expressed there (arrows in Figure 3B). As in the adult, a sharp boundary between these Hth-positive ommatidia and the rest of the eye was always observed.

Hth expression spanned the entire rim of the dorsal compartment (Figure 3C). This contrasts with the more restricted DRAs that have been described for most insect species (Labhart and Meyer, 1999). In most of the cases, Hth expression was excluded from the dorsal equatorial ommatidia (arrow in Figure 3C). In fact, these ommatidia at the equator are made of cells that come from both dorsal and ventral compartments.

Coordinated inner PR rhodopsin expression in the main part of the fly retina results from an instructive signal from R7 to R8 (Chou et al., 1996, 1999; Papatsenko et al., 1997). We therefore assessed whether a signal from R7 cells was needed in the DRA for the underlying R8 cells to differentiate properly by analyzing the expression of Hth and Rh3 proteins in the adult heads of *sevenless* (*sev*) mutants; the DRA R8 developed normally in these flies that lacked all R7 cells (Figure 3D), with Hth and Rh3 being limited to the R8 cell that also exhibit an enlarged rhabdomere diameter (Figure 3E). Therefore, unlike in the main part of the retina, no inductive signal from R7 cells is needed for the DRA R8 cells to correctly differentiate.

The R8 cells of the DRA represent a special cell type as indeed they lacked expression of the transcription factor Senseless that is expressed by all other R8 cells (*sens*; Frankfort et al., 2001; Figure 3F). Taking into account that these DRA R8 cells also expressed an otherwise R7 opsin (Rh3) and manifested morphological features not found in non-DRA R8 cells, like the enlarged rhabdomere diameter or the distal position of their nucleus (Figures 3F and 3G), it appears that R8 cells in the DRA are highly atypical. In contrast, we found that DRA R7 cells highly resemble the regular R7 cells. Although these cells also exhibited enlarged rhabdomeres, they expressed an R7 rhodopsin (Rh3) as well as the R7-specific markers Prospero (Figure 3H; Kauffmann et al., 1996; Cook et al., 2003) and their nuclei were located in the same layer as those of other R7 cells outside of the DRA (data not shown). The R8 cells of the DRA therefore represents a distinct inner PR cell fate, marked by expression of the inner PR marker Salm but lacking expression of both R7 (Pros) and R8 markers (Sens).

We used a constitutively activated form of Ras driven by the *sevenless* promoter (*sev*>RasVal[12]; Gaul et al., 1992) to induce extra R7 cells throughout the retina and assess whether these ectopic cells could make the decision to become DRA. Multiple Hth-positive cells were observed in the DRA of *sev*>RasVal12 pupae (Fig-
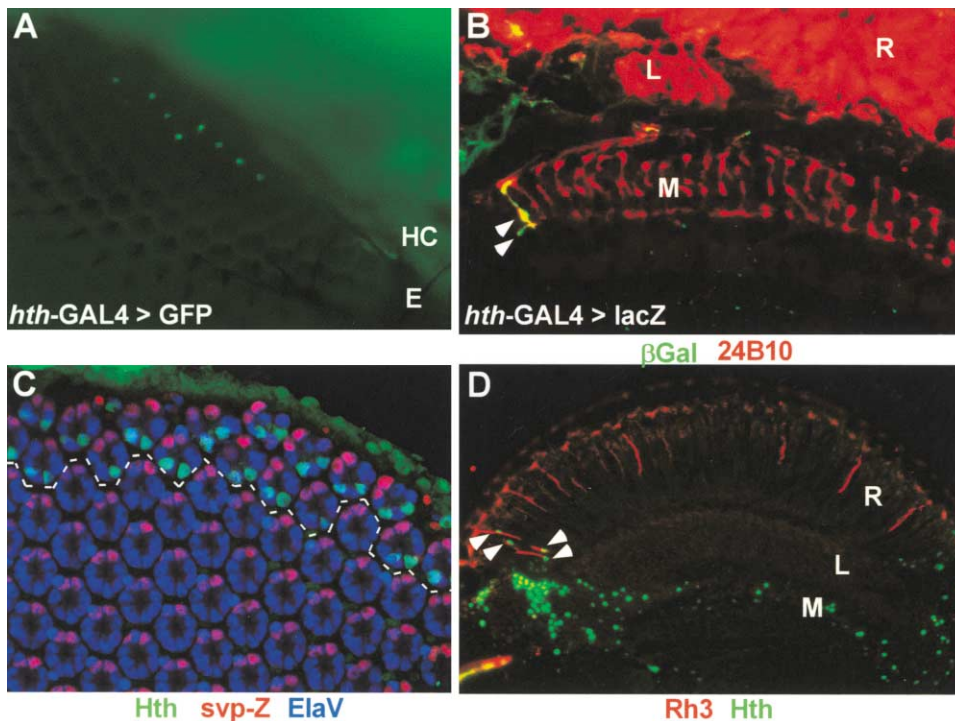
Figure 2. Inner PRs of DRA Ommatidia Express Homothorax

(A) Expression of *hth*-GAL4 in living flies: Individual ommatidia in the DRA of a living fly were visualized using cornea neutralization. *hth*-GAL4 combined with UAS-*eGFP* allowed detection of GFP expression in one row of ommatidia along the dorsal rim (HC, head cuticle; E, eye).

(B) Axonal projections of *hth*-GAL4 positive cells to the optic lobe: Frozen sections (10 μm, dorsal left) through adult heads of flies carrying both *hth*-GAL4 and UAS-lacZ transgenes were double-labeled with the PR marker 24B10 (red) and lacZ (green) revealing axonal projections of PRs to both the R8 (top white arrow) and R7 (bottom arrow) of the dorsal medulla.

(C) Pupal expression of Hth: Flat mounted pupal retinas (~48 hr APF) were dissected from *svp-lacZ* flies. Triple labeling of ElaV (blue), Hth (green), and β-Gal (red) showed expression of Hth in two rows of ommatidia at the dorsal rim. The *svp-lacZ* landmark (weak expression in R1 and R6; strong expression in R3 and R4) revealed Hth expression to be specific to R7 and R8 cells with a sharp boundary between DRA and non-DRA ommatidia (dashed line).

(D) Coexpression of Hth and Rh3 in adult DRA inner PRs: Frozen sections (dorsal left) showed Rh3 (red) and Hth (green) coexpressed in DRA inner PRs (arrows).

ure 3I, left) as well as in the adult (Figure 3I, right). As expected, all Hth-positive cells, except for one (the R8 cell), also coexpressed Pros (Figure 3I, left). Multiple Pros-positive cells per cluster were also observed outside of the DRA, but lacked Hth expression. As in the wild-type, only one or two rows of DRA ommatidia were found (Figure 3I, left). Virtually identical results were obtained by forcing the development of extra R7 cells in *seven-up* mutant clones (Mlodzik et al., 1990; data not shown). Similarly, when multiple R8 cells were induced in *rough* mutants (*ro^X63^*), Hth was expressed in multiple R8 cells in the DRA (data not shown).

Therefore, R7 or R8 always choose the DRA fate independently from each other when they are located in close proximity to the dorsal head capsule.

Homothorax Is Sufficient to Induce DRA Ommatidia
We tested a potential role of *hth* in controlling cell fates in the DRA by assessing whether its expression is sufficient to induce DRA development. We misexpressed Hth in all developing PRs posterior to the morphogenetic furrow using UAS-*hth* (Ryoo et al., 1999) under the control of GMR-GAL4 (GMR>*hth*; Moses and Rubin, 1991). Rh3 expression was expanded to all inner PRs throughout the retina (Figure 4A) while all other inner PR rhodopsins

(Rh4, Rh5, and Rh6) were lost (Figure 4D). Expression of the outer PR opsin was not affected as shown by a *rh1*-GFP transgene (Pichaud and Desplan, 2001) (Figure 4C). Additionally, expression of the R8 marker Sens was totally lost (data not shown). We also visualized *rh3* expression in living flies using a *rh3*-GFP transgene and corneal neutralization (Franceschini and Kirschfeld, 1971); *rh3*-GFP expression was expanded to all ommatidia in GMR>*hth* flies (data not shown). A *rh3*-lacZ transgene allowed us to show that all inner PRs projected to the medulla (Figure 4B). Although the morphology of the medulla was somewhat disturbed, both R7 and R8 termination layers could be distinguished. The outer PRs projected correctly to the lamina and never expressed *rh3*.

The rhabdomere diameter of all inner PRs was considerably enlarged in GMR>*hth* flies (Figures 1F and 4E). As a significant number of these inner PR rhabdomeres had morphological problems, we analyzed them by electron microscopy. Cross-sections of some inner PR rhabdomeres exhibited a kidney-like shape (Figure 4F, top) and some were split in two (data not shown). However, the area of inner PR rhabdomere cross-sections was always enlarged.

Therefore, expression of Hth is sufficient to force any inner PR into choosing the fate of a polarization-sensi-
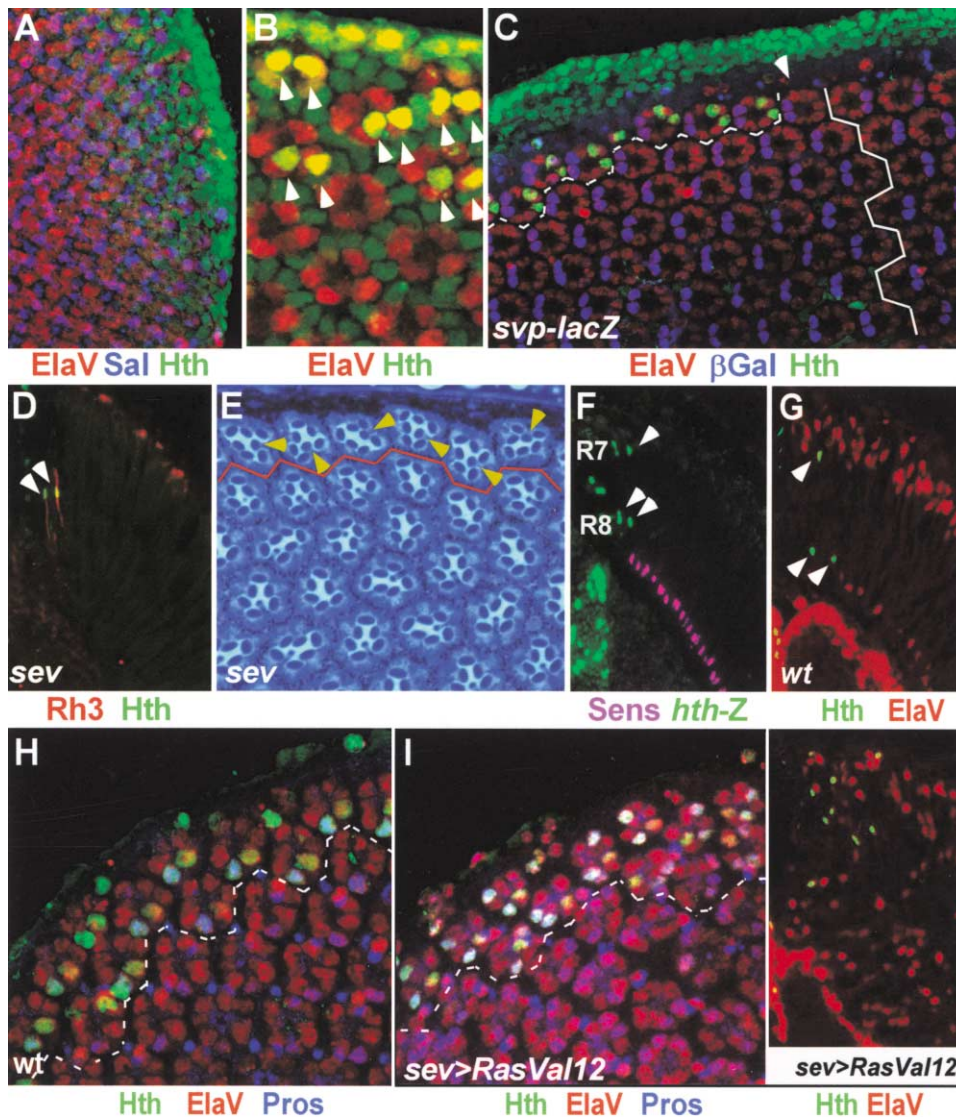
Figure 3. Development of the DRA

(A) Whole-mounted larval third instar eye disc (anterior left) stained with antibodies against Hth (green), Salm (blue), and ElaV(red). At this stage, Hth was detectable in nonneuronal posterior cells but not in PRs. Salm was already expressed in R7 and R8.

(B) Early flat-mounted pupal retina. Double labeling with ElaV (red) and Hth (green) revealed two rows of DRA ommatidia with inner PRs coexpressing Hth and ElaV (arrows) and additional Hth staining in pigment cells surrounding all PR clusters.

(C) The DRA does not cross the eye equator: flat-mounted pupal retina (∼48 hr APF) dissected from *svp*-lacZ flies. Triple labeling of ElaV (red), Hth (green), and βGal (blue) revealed one row of developing DRA ommatidia (dashed line) in the dorsal half of the eye, stopping one cluster before the equator (white line).

(D) DRA R8 develop normally in *sevenless* mutants: frozen section (10 μm, dorsal left) of a *sev* mutant. Double labeling of Rh3 (red) and Hth (green) identified the DRA in the two dorsalmost rows of R8 cells (arrows).

(E) Rhabdomere morphology of *sevenless* mutants: epon thin section through the dorsalmost part of an adult *sev* eye at the level of R8. The R8 cells exhibited enlarged rhabdomere diameters (arrows) with a sharp boundary between DRA and non-DRA ommatidia (red line). Mispositioning of R8 cells within the ommatidial cluster was observed as previously reported (Campos-Ortega et al., 1979).

(F) Exclusion of the R8 marker Senseless from the DRA: frozen sections (dorsal left) of adult *hth-lacZ* flies. Double labeling with Senseless (pink) and Hth-lacZ (green) revealed exclusion of Sens expression from DRA R8 cells as well as the elevated position of their nuclei (arrows).

(G–I) Induction of multiple R7 cells in the DRA. (G) Frozen sections of control adult flies (dorsal left): double labeling of ElaV (red) and Hth (green) revealed 2–4 Hth-positive inner PR nuclei per section. (H) Flat-mounted pupal retinas (∼48 hr APF) dissected from *yw* flies labeled for ElaV (red), Hth (green), and Pros (blue). Within the DRA (dashed line) both inner PRs (R7 and R8) stained for Hth. One of these cells (R7) coexpressed Pros (white cells) whereas R8 did not express this R7 marker (yellow cells). In flies expressing activated Ras driven by the *sev* promoter (sev>RasVal12), multiple Pros-positive cells per cluster were obtained throughout the retina (I, left). Within the DRA, multiple cells (3–4) expressed Hth (green), with all except one (R8, yellow cell) coexpressing Pros (white cells). Therefore, extra R7 cells born within the DRA always chose the DRA R7 cell fate. This situation was maintained until adulthood (I, right); an increased number (7–9/section) of Hth positive cells were observed compared to an average of 3 in wt (see G).
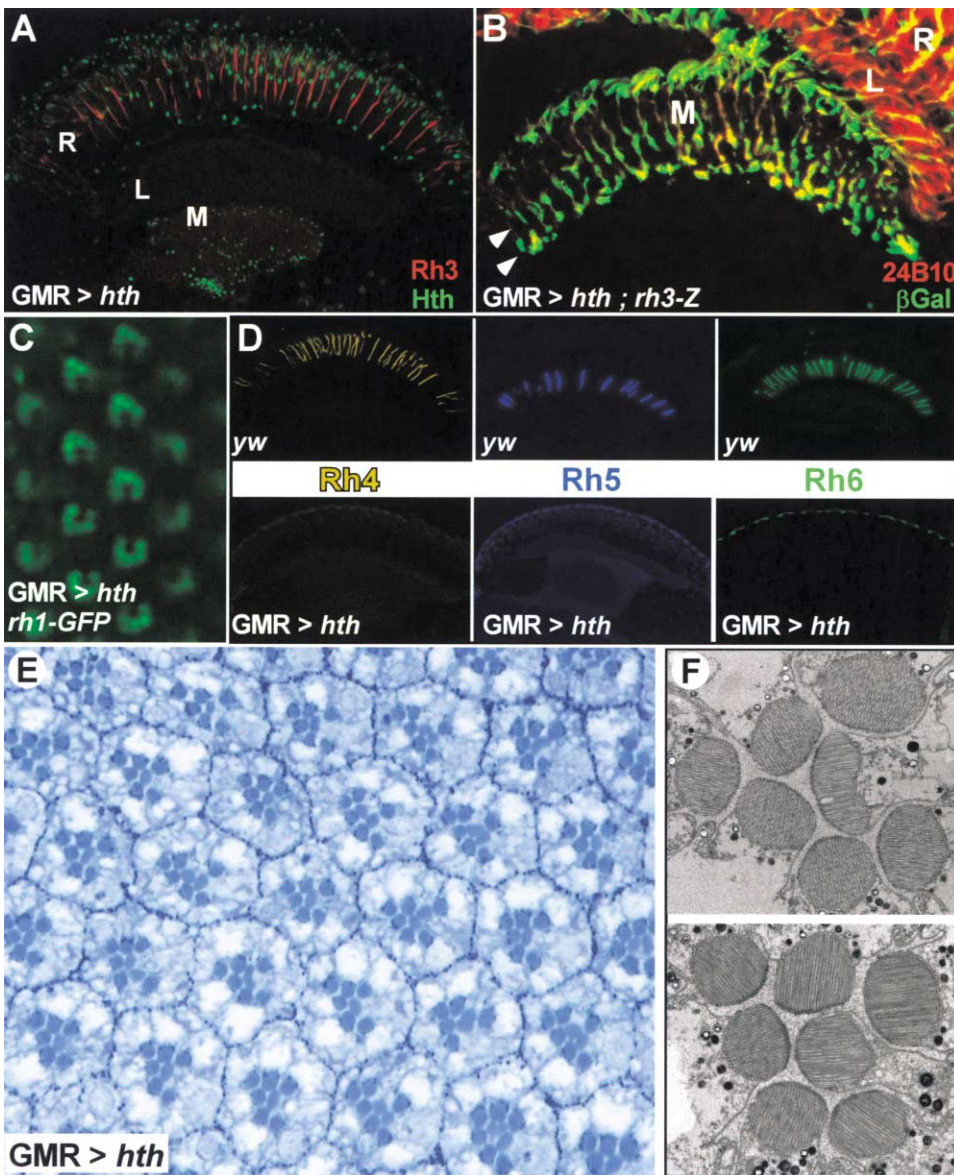
Figure 4. Homothorax Is Sufficient to Induce the DRA Fate in Inner PRs

(A) Overexpression of *hth* expands Rh3 expression: frozen section (dorsal left) of adult flies overexpressing *hth* under the control of "long" GMR-GAL4 (GMR>*hth*; see Experimental Procedures). Hth (green) and Rh3 (red) were coexpressed in all inner PRs.

(B) Axonal projections of *rh3* expressing fibers to the optic lobes: frozen sections (dorsal left) of adult GMR>*hth* flies carrying *rh3*-lacZ transgenes. All inner PRs projecting to the medulla expressed the DRA opsin *rh3* (24B10 is red and anti-βGal is green). Projections to both R7 and R8 layers (white arrows), but not to the lamina were observed, suggesting that all inner PRs were driven into the DRA fate.

(C) Outer PRs are not transformed by *hth*; expression of *rh1*-eGFP observed with water immersion was not affected in live GMR>*hth* flies.

(D) Overexpression of Hth results in loss of *rh4*, *rh5*, and *rh6* expression: frozen sections of adult control flies stained for Rh4, Rh5, and Rh6. Expression of these non-DRA inner PR rhodopsins was lost in GMR>*hth* flies (bottom).

(E) Expression of Hth is sufficient to ectopically induce DRA morphology. Epon thin section through ommatidia near the equator in GMR>*hth* flies showing that all ommatidia exhibited DRA morphology (compare with Figure 1F), exhibiting enlarged inner PR rhabdomeres.

(F) Rhabdomere morphology in ectopic DRA ommatidia. Electron microscopy revealed occasional malformations, like kidney-shaped inner PR rhabdomeres (top) in GMR>*hth* flies, although most ommatidia were virtually identical to normal DRA ommatidia (bottom, compare Figure 1E).

tive DRA cell. Outer PRs cannot be transformed into DRA inner PRs.

**Loss of Homothorax Results in Loss
of Dorsal Rim Area**
To test the function of *hth* in DRA development, we induced mitotic clones (Xu and Rubin, 1993) homozy-

gous for the hypomorphic mutation *hth*[B2]. Ommatidia located in *hth*[B2](−/−) clones touching the DRA lost their typical enlarged inner PR rhabdomeres (Figure 5A, compare black and yellow arrows). Because Hth is important for cell proliferation anterior to the MF, only small clones could be recovered (Bessa et al., 2002). We thus overexpressed a dominant-negative Hth containing the Exd-
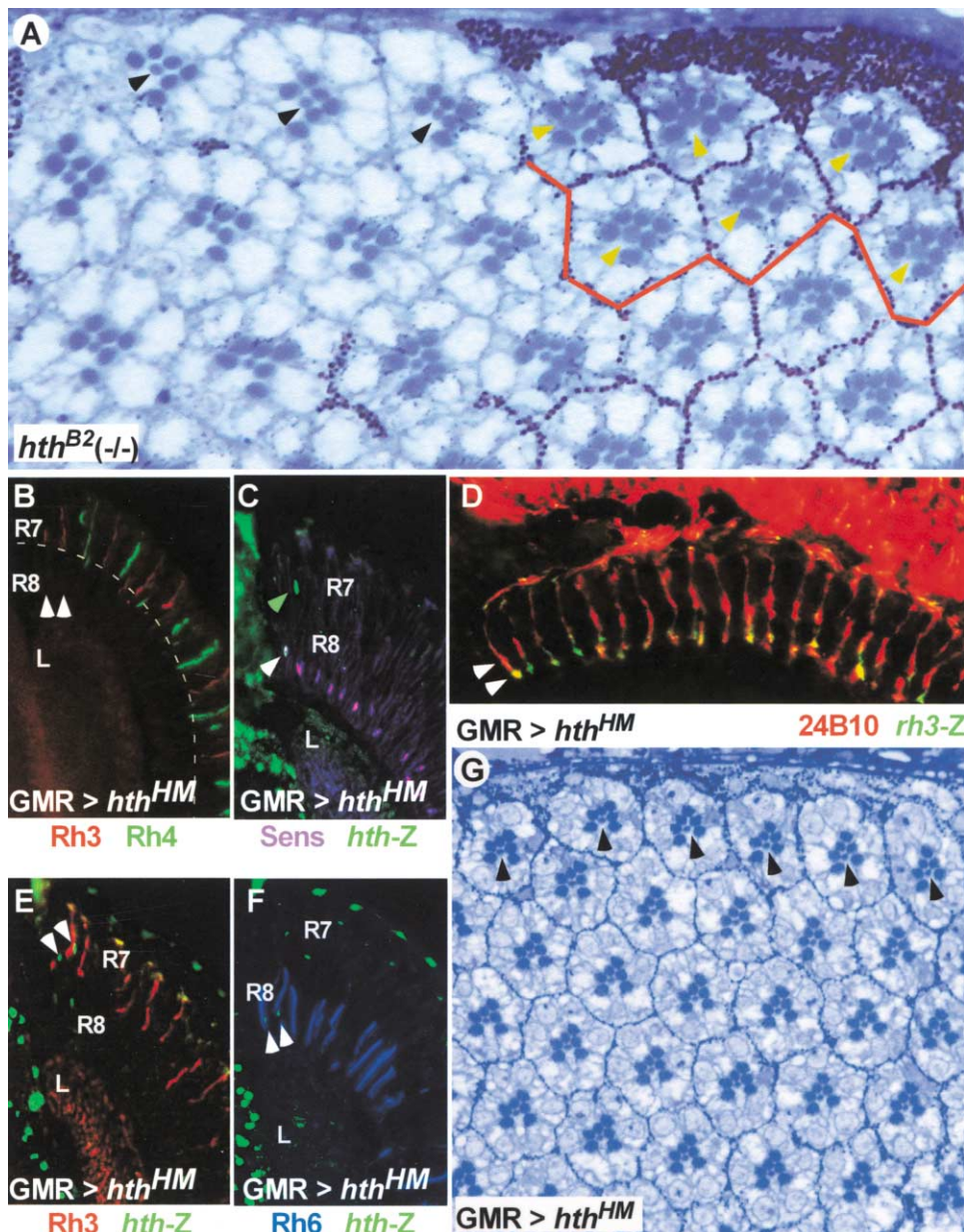
Figure 5. Loss of Hth Leads to a Loss of the DRA

(A) Loss of *hth* leads to a loss of DRA morphology: Epon thin section of eye tissue homozygous for the *hth^B2* hypomorph (unpigmented tissue, left). Mutant ommatidia (black arrows) located at the dorsal eye rim lost the enlarged inner PR rhabdomere phenotype (yellow arrows in wt tissue).

(B–D) Dominant-negative HthHM leads to loss of DRA fate in R8 cells. Frozen section of adult flies overexpressing HthHM under the control of "long" GMR-GAL4.

(B) Double labeling of Rh3 (red) and Rh4 (green) revealed a loss of Rh3 expression in R8 cells of the DRA (white arrows).

(C) Double labeling of *hth*-lacZ (green arrows) and Sens (pink) in GMR>*hthHM* flies revealed that R8 cells in the DRA maintain Sens expression (white arrow) and that the position of their nuclei is almost at the same level as those of non-DRA R8 (compare Figure 3F).

(D) Projections of *rh3*-lacZ expressing cells to the R8 layer in the medulla is lost in GMR>*hthHM* flies. Double labeling of lacZ (green) and the PR marker 24B10 (red) revealed no projections of the dorsalmost fibers to the R8 layer (top arrow) whereas rh3-lacZ fibers were still observed in the corresponding R7 layer (bottom arrow) indicating that R8 cells clearly lost the DRA fate.

(E and F) Loss of Hth transforms the DRA into atypical color-sensitive ommatidia: double labeling of the DRA (*hth*-lacZ) and inner PR opsins in frozen sections of adult GMR>*hthHM* (dorsal left). DRA R7 cells marked by lacZ expression (E, arrows) still expressed Rh3 (red), but the underlying R8 cells marked by lacZ (F, arrows) always expressed Rh6 (blue) suggesting that loss of *hth* function leads to transformation of the DRA into a color-sensitive eye region containing atypical Rh3/Rh6 ommatidia.

(G) *hthHM* leads to loss of DRA morphology: epon thin sections through adult GMR>*hthHM* eyes revealed that DRA inner PRs had lost their enlarged rhabdomere size (compare Figure 1F). GMR>*hthHM* eyes lack a specialized DRA but are otherwise normal.

interacting "HM domain" but lacking the entire homeo-domain (*hthHM*; Ryoo et al., 1999). Adult flies expressing HthHM under GMR control (GMR>*hthHM*) exhibited no ob-vious external eye phenotype (data not shown). As ex-pected, HthHM could not transform inner PRs into DRA and expression of all inner PR rhodopsins appeared

normal outside of the DRA (data not shown). In the DRA however, Rh3 was no longer expressed in R8 cells (Figure 5B, white arrows), suggesting a loss of DRA, at least in the R8 cell layer. A *lacZ* enhancer trap insertion in *hth* was introduced to mark the DRA in GMR>*hth*[HM] flies. R8 cells in the DRA are a specialized cell type because they express neither the R8 marker Senseless (Sens) nor the R7 marker Prospero (Pros). However, *hth*-lacZ and Senseless were coexpressed in the presence of GMR>*hth*[HM] (Figure 5C, both arrows). Additionally, the nuclei of DRA R8 cells were now located significantly more basal (white arrow) as is typical for regular R8 cells. This further suggested that R8 cells had lost DRA identity and chosen the regular R8 cell fate. Furthermore, no projections to the R8 cell layer of the medulla could be observed with *rh3*-lacZ (Figure 5D, top arrow), whereas *rh3*-lacZ expressing R7 terminations remained (bottom arrow). To assess whether *rh3*-expressing R7 cells of GMR>*hth*[HM] flies had lost their DRA identity, we analyzed inner PR rhabdomere morphology of these flies. All central PR cells (R7 and R8) at the dorsal rim had lost their typical large rhabdomere (Figure 5G). Furthermore, all DRA R7 cells retained Rh3 expression (Figure 5E) while their R8 counterparts exclusively expressed Rh6 (Figure 5F), resulting in DRA ommatidia with an "odd-coupled" Rh3/Rh6 expression. Rh4 or Rh5 were never found to be expressed in the DRA of these flies (data not shown). In wt flies, a low ratio (∼6%) of "atypical" odd-coupled Rh3/Rh6 ommatidia exists outside of the DRA, whereas R4/Rh5 ommatidia never occur (Chou et al., 1996). Therefore, dominant-negative Hth prevents DRA development, transforming it into an atypical color-sensitive eye region.

This led us to conclude that *hth* is necessary for inner PRs in the DRA to induce development into polarization detectors. Loss of Hth function always results in the formation of atypical color-sensitive (Rh3/Rh6) ommatidia rather than **p** or **y** subtypes.

The Role of Dorsal Selector Genes in DRA Formation

Although the *IRO-C* complex is required to specify the dorsal region of the eye imaginal disc and *mirr*, *ara*, and *caup* are expressed dorsally anterior to the morphogenetic furrow (Cavodeassi et al., 2001), no role has yet been assigned to these genes in developing PRs posterior to the MF. Since the DRA is restricted to the dorsal retina, we tested whether the *IRO-C* complex played a role in its development. We first tested whether *IRO-C* genes were expressed in PRs at the time of *hth* expression by using several available *IRO-C lacZ* enhancer trap lines. In the adult, *caup-lacZ* (rF209) exhibited strong expression in all cells of the dorsal retina (Figure 6A), while expression of several insertions in *mirr* was not detectable at this stage. Such differences in the expression of *ara* and *caup* versus *mirr* have previously been reported (Pichaud and Casares, 2000). rF209 (*caup*) expression was much weaker but still present in dorsal PRs at ∼48 hr APF, resulting in coexpression with Hth (Figure 6B). Expression was not uniform and was strongest in the most dorsal ommatidia and faded away few rows away from the dorsal cuticle; it returned to high levels of expression in the adult. Therefore Caup (and

maybe Ara), but not Mirr, are expressed at later stages of PR development than previously detected.

We induced clones of eye tissue homozygous for a deletion covering all three genes (DMF3). However, some inner PRs clearly exhibiting DRA rhabdomere morphology were observed in these clones (data not shown) and Hth expressing inner PRs were frequently observed in *IRO-C*[DFM3] (−/−) clones spanning the DRA (Figure 6C, arrowheads). As the available *IRO-C* deletions might not fully remove all *IRO-C* function, we also tested whether the genes of the *IRO-C* complex were sufficient to induce DRA development. We misexpressed each of them, alone or in combination, in the eye, using GMR-GAL4. Although high levels of expression led to strong eye disruption, low levels of either Ara (GMR>*ara*), Caup (GMR>*caup*), or Mirr (GMR>*mirr*) were sufficient to induce ectopic ventral rim areas: Hth expression was detectable in one or two rows of ommatidia, in inner PRs all around the pupal retina (∼48 hr APF; Figure 6D). Using *svp*-lacZ in GMR>*ara* flies, we showed that Hth expression was expanded into the ventral half of the retina (Figure 6E), including the equatorial ommatidia. As in the DRA, adult ommatidia in this induced ventral rim area expressed Rh3 in both R7 and R8 cells (Figure 6F).

We conclude that dorsal expression of some *IRO-C* genes persists until adulthood and although they might not be absolutely necessary, a single *IRO-C* gene is sufficient to induce DRA development in all marginal PRs posterior to the MF.

The DRA Develops in Response to *wingless* Signaling

Since the DRA forms near the head cuticle where *wingless* is expressed, we tested whether activation of the *wingless* pathway was involved in DRA development. We overexpressed an activated form of the *wingless* effector Armadillo (Arm[S10]) in all developing PRs posterior to the MF. These GMR>ArmS10 flies had rough eyes, with some ommatidia losing PRs when strong drivers were used (see Experimental Procedures). However, *hth* and *rh3* expression was dramatically expanded into many inner PRs throughout the dorsal adult retina (Figure 7A). In pupal retinas (∼48 hr APF), Hth was clearly expanded to the entire dorsal half of the eye (Figure 7B) stopping at the equator and often leaving one dorsal row unmarked (Figure 7C), a situation similar to what we observed for the much more restricted DRA of wt flies.

We tested whether DRA cells responded directly to Wg signaling by overexpressing a dominant-negative form of TCF/pangolin, the transcriptional effector of the *wingless* pathway (UAS-TCFΔN). Depending on the strength of the GMR driver used, adult GMR> TCFΔN flies had eye phenotypes ranging from wild-type to very rough, but DRA development was normal in all flies analyzed, as visualized by the normal expression of Rh3 and Hth in the DRA (Figure 7D). We also induced mitotic clones of eye tissue lacking both Wg receptors, Fz and DFz2 (Chen and Struhl, 1999). Only very few and very small clones were obtained but, similarly to GMR>TCFΔN, no loss of Hth expression was observed at the DRA (Figure 7E). Finally, we induced larger homozygous clones of a null allele of *disheveled* (*dsh*[V26]), an essential component
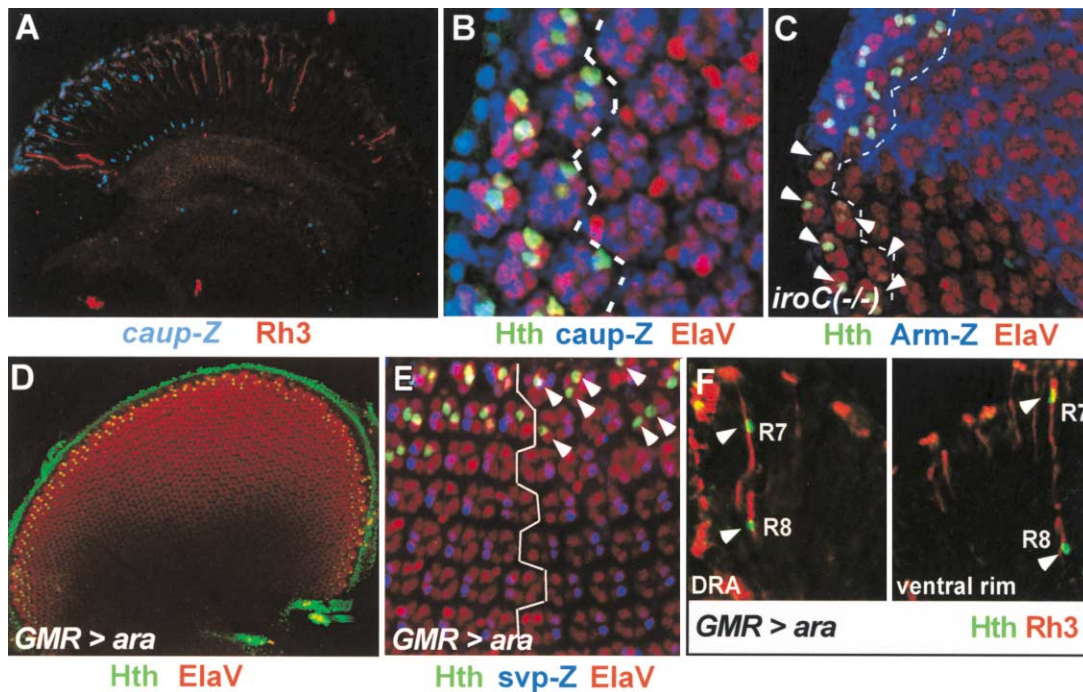
Figure 6. Dorsal Selector Genes Induce the DRA

(A) Adult expression of *caup*-lacZ: frozen section (dorsal left) of adult heads of flies carrying the caup (rF209) enhancer trap were double-labeled for Rh3 (red) and βGal (blue) and revealed strong lacZ expression throughout the dorsal region of the eye.

(B) Weak pupal expression of *IRO-C* genes: flat-mounted pupal retina (∼48 hr APF) dissected from flies carrying the caup (rF209) insertion. Triple labeling against ElaV (red), Hth (green), and βGal (blue) revealed weak rF209 expression in all PRs of dorsal ommatidia, fading toward the equator but clearly coexpressed with Hth in the developing DRA ommatidia (dashed line).

(C) Loss of *IRO-C* complex does not lead to loss of Hth expression: flat-mounted pupal retina (∼48 hr APF) from flies with clones of tissue homozygous for DMF3 labeled by the absence of Arm-lacZ (shown in blue). Triple labeling of ElaV (red), Hth (green), and βGal (blue) revealed that Hth expression (arrows) persisted in DMF3($^{-/-}$) clones located in the DRA (dashed line).

(D and E) Expression of *IRO-C* genes is sufficient to induce DRA: (D) flat-mounted pupal retina (∼48 hr APF) from "short" GMR-GAL4/UAS-ara (GMR>*ara*). Double labeling of ElaV (red) and Hth (green) revealed DRA formation all around the developing eye. (E) DRA-specific Hth expression clearly crossed the equator (arrows) identified by *svp*-lacZ (blue) and expanded to the ventral rim area.

(F) Misexpression of *IRO-C* genes induces ventral rim areas (VRA): frozen section (dorsal left) of adult short GMR>*ara* flies. Double labeling of Rh3 (red) and Hth (green) revealed the presence of DRA (left) as well as an unusual VRA (right), with both R7 and R8 cells coexpressing Hth and Rh3 (white arrows).

of Wingless signaling. Eye morphology was visibly affected resulting in large clonal outgrowths due to the loss of inhibition of MF progression. Although Hth expression was sometimes partially lost in small clones, it clearly persisted in the large clones and in several cases more than two additional DRA rows were detected in the adjacent wt tissue that expanded into the head cuticle (Figure 7F).

Together, these data indicate that ectopic activation of the *wg* pathway is sufficient to induce DRA development dorsally, but reception of the Wg signal in PRs is not absolutely necessary for DRA development to proceed, suggesting the possible involvement of a redundant DRA inducing factor and/or additional Wnt receptor pathway(s)

Discussion

Homothorax Provides New Insights into PR Development

We have shown that Homothorax specifies the PRs that provide input to the polarization compass by distin-

guishing them from prospective color-sensitive PRs. At the onset of pupation, the inner PRs R7 and R8 along the dorsal rim specifically turn on expression of Hth and maintain it through adult life. This late onset of Hth expression is particularly interesting since a gradient of PR maturation still exists at these early pupal stages: ommatidial clusters have continuously been recruited by the progressing MF and therefore, differ in age by several days. It is unclear why specification of DRA ommatidia by Hth does not occur immediately posterior to the MF, especially as Wg is already expressed at the dorsal and ventral poles of the imaginal disc. A temporal trigger such as the pulses of ecdysone occurring at the onset of metamorphosis might be required to induce Hth expression.

The role of Hth in DRA development represents a specific example illustrating how late PR differentiation events specify the three ommatidial subtypes. It provides further evidence that establishment of terminal PR fates in **p, y,** or DRA ommatidia is achieved by consecutive determination steps. In this model, early PR cell fate decisions (i.e., determination of the 8 types of PRs) and
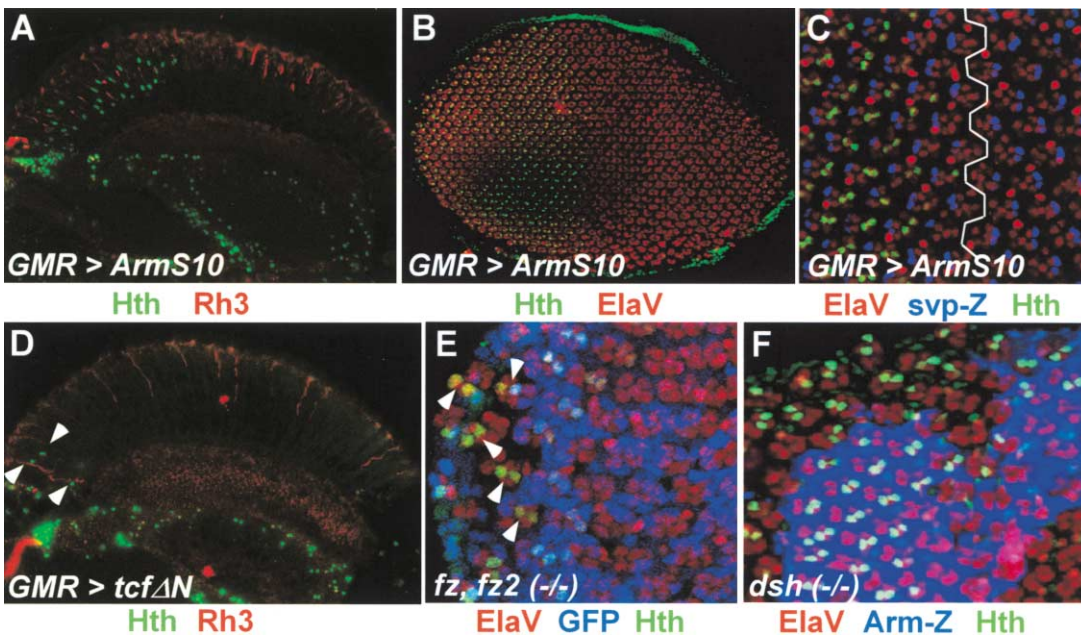
Figure 7. Hth Induces the DRA in Response to *wingless*

(A–C) Activation of the *wingless* pathway transforms all dorsal PRs into DRA. (A) Frozen section (dorsal left) of flies overexpressing activated Armadillo (ArmS10) under long GMR-GAL4 control. Double labeling of Rh3 (red) and Hth (green) revealed a dramatic expansion of the DRA throughout the dorsal eye. Rh3 was the only inner PR opsin expressed in the dorsal eye. (B) Flat-mounted pupal retinas (∼48 hr APF) from GMR>ArmS10 flies were double-labeled against ElaV (red) and Hth (green). Hth expression spanned the entire dorsal half of the developing eye. (C) Introduction of *svp*-lacZ (blue) showed that Hth expression almost reached the equator (white line), most of the times being excluded from the equatorial ommatidia.

(D–F) DRA ommatidia do not directly respond to *wingless*. (D) Frozen section (dorsal left) of flies overexpressing a dominant-negative form of Dtcf (*pangolin*) using short GMR-GAL4 (GMR>DtcfΔN). Double labeling of Rh3 (red) and Hth (green) revealed that the DRA remains unaffected in these flies (arrows). (E) Flat-mounted pupal retinas (∼48 hr APF) from flies with small homozygous clones mutant for both *wg* receptors Fz and Fz2 (*fz*^{H51} *fz2*^{C1} $^{-/-}$): triple labeling of Hth (green) and ElaV (red) in clones marked by loss of a ubiquitin-GFP transgene (shown in blue) revealed that Hth expression was not lost in *fz*^{H51} *fz2*^{C1} (white arrows). (F) Larger homozygous mutant clones of a null allele of *disheveled* (*dsh*), marked by the absence of Arm-lacZ (shown in blue) were analyzed in pupal retinas (∼48 hr APF). Triple labeling with Hth (green) and ElaV (red) revealed that DRA-specific Hth expression persisted in *dshV26*$^{-/-}$ mutant tissue (top). Additional DRA rows appeared in wt tissue adjacent to *dshV26* clones (center) probably due to overproliferation.

projection to the optic lobes occur in the third instar imaginal disc. The distinction between inner and outer PRs is controlled by *spalt*: Salm represents the earliest marker expressed in both R7 and R8 starting at third instar larval stages (Figure 3A) and maintained to adulthood. Loss of both *salm* and *salr* results in transformation of adult inner into outer PRs; the inner PR rhodopsin genes (*rh3-rh6*) are replaced by the outer PR *rh1*, although most axons still maintain their projections to the medulla (Mollereau et al., 2001). R7 and R8 are further distinguished from each other by expression of Prospero and Senseless, respectively. The distinction between the three classes of ommatidia appears to be achieved later; *hth* expression in the DRA is only initiated during early pupation. We propose that only those cells that express Sal are competent to face another cell fate decision at the beginning of pupation. The inner PRs of ommatidia close to the dorsal rim come under the influence of a DRA inducing signal that includes Wg and express Hth, whereas in all other ommatidia two different pairs of color-sensitive PRs develop in a stochastic manner. Consistent with this model, the outer PRs, which do not express Sal, are not transformed by forced expression of Hth, and Hth expression is lost in *salm, salr* double mutants. The crucial decision made

by inner PRs between color sensors or polarization detectors therefore depends uniquely on their position within the retina.

Homothorax Is the Key Regulator of DRA Development

Inactivation of Hth function results in the transformation of the DRA into atypical color-sensitive ommatidia expressing Rh3 in R7 and Rh6 in R8. Overexpression of both activated Armadillo and dominant-negative Hth (GMR>ArmS10+*hth*^{HM}) also results in all dorsal R7 cells expressing *rh3* and all underlying R8 cells expressing *rh6* (data not shown). This further suggests that Wg activity directs the inner PRs toward a DRA program but that without Hth function, the DRA program cannot be executed: inner PR rhabdomeres do not become larger and Rh3 is not expressed in R8. But why are atypical color-sensitive Rh3/Rh6 ommatidia always formed? Loss of Hth might not allow the full program of color PR specification to be activated at the dorsal rim as **p** and **y** subtypes are not distinguished stochastically. R7 always choose expression of *rh3*; R8, which are not properly instructed by R7, choose *rh6* and not coupled expression of *rh5*. These results are consistent with the model that Rh6 is the ground state for R8, since in the

absence of R7 (*sev*) the vast majority of R8 express Rh6 (Chou et al., 1996; Papatsenko et al., 1997). By extrapolation, *rh4* was therefore suggested to be the ground state in R7 (Chou et al., 1999). However, our results suggest that Rh3 might in fact represent the ground state in R7. We have indeed recently identified a gene that is both necessary and sufficient for the expression of Rh4 in R7, presumably by distinguishing **y**R7 (*rh4*) from the ground state **p**R7 (*rh3*; M.F.W. and C.D., unpublished data). We therefore propose that the Rh3/Rh6 pair represents the combination of independent R7 and R8 "ground states" upon which PR subtype decisions are imposed; the stochastic choice made by R7 outside the DRA is usually linked to communication from R7 to R8, resulting in coupling of *rh3/rh5* in **p** and *rh4/rh6* in **y** subtypes. It appears that this process is suppressed in DRA inner PRs, even when Hth function is lacking, suggesting that the high Wg levels activating Hth at the dorsal rim might also repress the subtype decisions of color-sensitive ommatidia as well as communication between R7 and R8.

Expression of Hth in inner PRs is sufficient to induce the DRA fate both morphologically (increase in rhabdomere diameter) as well as molecularly (monochromacy by expression of Rh3 in both R7 and R8 and repression of Sens in R8), although the genetic programs activated by Hth remain unknown. One of the major roles of Hth is to translocate Exd into the nucleus (Rieckhof et al., 1997) where they form transcriptional complexes with HOX proteins. Consistent with this, we found that Exd is localized to the nuclei in inner PRs of the DRA, but not in color-sensitive ommatidia, suggesting that Hth and Exd function together. We are currently testing whether Hth and Exd directly repress Sens in R8 cells of the DRA, since loss of Sens expression seems to be essential for DRA R8 cells to escape the typical color-sensitive R8 fate and for switching to the DRA R8 fate with its R7-type *rh3* expression. A better understanding of Hth function in vivo is of great importance as mammalian homologs of Hth (Meis1a) cooperate with HOX factors to induce acute myeloid leukemia (Moskow et al., 1995) although direct association with HOX factors might not always be necessary. Since no HOX proteins have been implicated in *Drosophila* eye development, DRA development represents an attractive model system for identifying new factors interacting with Hth and Exd in vivo.

Late Dorsoventral Patterning of the Retina
Although the *IRO-C* genes have been suggested to act only before the MF (McNeill et al., 1997), our experiments now reveal that *IRO-C* genes are able to induce dorsal-specific morphological changes at later time points. We provide evidence that members of the *IRO-C* complex indeed act as selector genes to specify the dorsal compartment of the developing eye. They fulfill at least two additional typical features proposed for such selector genes: persistence of expression and induction of transformations when misexpressed in the ventral compartment.

caup persists at very low levels during pupal stages before returning to high levels in adults. One possible explanation for such transient downregulation could be that high levels of *IRO-C* genes are toxic for the developing PRs. Indeed, we observe massive cell death when we overexpressed *ara*, *caup*, or *mirr* under the control of a strong GMR-GAL4 driver. Weaker drivers expressed posterior to the MF, however, give rise to healthy PRs and a ventral rim area. Therefore, during early pupal stages, low levels of dorsally expressed *IRO-C* genes might restrict induction of Hth expression to the dorsal half of the rim. Our results suggest that the *IRO-C* complex acts together with a factor induced by high levels of Wg signaling. Indeed, overexpression of both ArmS10 and *ara* posterior to the morphogenetic furrow induces Hth expression in inner PRs throughout the eye. Since loss of all three *IRO-C* genes does not result in a loss of the DRA, a fourth unknown factor might be partially redundant with the *IRO-C* genes, or alternatively the deficiency used to eliminate the three genes might bear residual activity (H. McNeill, personal communication).

Although activation of the Wg pathway strongly induces DRA throughout the *IRO-C* compartment, the DRA develops normally when *Fz* and *DFz2*, *dsh*, or *TCF* are inactivated (Figures 7D, 7E, and 7F). It is possible that low levels of wild-type protein persist long enough in the clones for DRA development to proceed, although this is unlikely considering the late onset of Hth expression. Therefore, redundant factors might exist, such as the Derailed receptor which has recently been shown to mediate Wnt5 function (Yoshikawa et al., 2003). Alternatively, another diffusible factor could act in parallel with the Wg/Fz pathway to induce the DRA, possibly acting downstream of Wg as a "relay signal." Indeed, cell nonautonomous inductive effects downstream of both *wg* and *Arm* have been reported to influence cell fate determination at the periphery of the fly retina, including the DRA (Tomlinson, in press).

In summary, *hth* is both necessary and sufficient for changing the function of PRs from color vision toward polarized light detection, thus switching the perception associated with a given PR subtype. Hth therefore represents an important tool to further understand how terminal PR differentiation processes depend on spatial cues as opposed to the stochastic choice between color-sensitive ommatidial subtypes in the main part of the fly retina. In the future, it will be interesting to understand how the molecular targets of *hth* affect DRA cell properties and to investigate how the eyes of different species adapted their PRs to respond best to different environments.

Experimental Procedures

Fly Stocks
GAL4 drivers
For all misexpression experiments, the strength and degree of PR specificity of the driver constructs used appeared to be crucial. We used two different transgenic lines for GMR-GAL4 (Moses and Rubin, 1991). One is the "short GMR," made of a pentamerized 29 bp glass binding site. We also generated a "long GMR" using a longer glass site with pentamerized 38 bp glass sites (B. Mollereau and C.D., unpublished data). Expression using such long GMR promoter is more PR specific and overexpression generally resulted in less dramatic eye phenotypes.

The following lines were generously provided by: UAS-GFP::hth, UAS-*myc::hth*, and UAS-GFP::hthHM (Ryoo et al., 1999); UAS-GFP::hthHM, UAS-*ara*, and UAS-*caup* (J. Modolell); UAS-*mirr* (H.

McNeill); UAS-*ArmS10* and UAS-*tcf∆N* (van de Wetering); UAS-GFP (M. W.), and UAS-*lacZ* (J. Treisman). *hth*-GAL4 *caup*^{rF209}-PZ and *hth*$^{l(3)06762}$-PZ (Bloomington Stock Center); and *svp*-PZ (U. Gaul). *ey*-Flip (B. Dickson); FRT80-*Arm-lacZ*, FRT2A-ubi-GFP, FRT19-*Arm*-lacZ, FRT82B-p[w+], FRT19-*dshV26*, and FRT82B-*roX63* (J. Treisman); FRT82B-*hthB2* and FRT82B-*hthP2* (R. Mann); FRT2A-*fz*^{H51} *fz2*^{C1} (G. Struhl); and FRT82B-*svp*^{E22} (U. Gaul). *sev>RasVal12* (Gaul et al., 1992); *rh3*-lacZ (Fortini and Rubin, 1990); *rh1*-GFP and *rh3*-GFP (Pichaud and Desplan, 2001).

Microscopy and Histology
GFP expression in photoreceptors of living flies was assessed by neutralizing the cornea using water immersion (Pichaud and Desplan, 2001). For transmission light and electron microscopy, the eyes were fixed with 2% glutaraldehyde (eventually with 1% OsO$_4$) in 0.05 M Na-cacodylate buffer [pH 7.2] for 2 hr at 4°C. Following postfixation with 2% OsO$_4$ in 0.05 M Na-cacodylate buffer [pH 7.2] for 2 hr at 4°C, the tissue was dehydrated with 2,2-dimethoxypropane and embedded in Epon 812. 1 μm sections for light microscopy were stained with methylene blue. Silver sections for electron microscopy were stained with uranyl acetate and lead citrate.

Immunohistochemistry
Primary antibodies used were anti-βGal rabbit 1/5000 (Cappel); anti-βGal mouse monoclonal 1/500 (Promega); anti-Hth guinea pig 1/500 (R. Mann); anti-ElaV mouse or rat monoclonals 1/10 (Iowa University Hybridoma bank); anti-24B10 mouse monoclonal 1/10 (L. Zipursky); anti-Pros mouse monoclonal 1/4 (C. Doe, Oregon); anti-Sens guinea pig 1/10; anti-Rh1 mouse monoclonal 1/10 (Iowa University Hybridoma bank); anti-Rh3 rabbit 1/10 (C. Zuker); anti-Rh3 chicken 1/20 (Cook et al., 2003); anti-Rh4 rabbit 1/300 (C. Montell); anti-Rh5 mouse monoclonal 1/100 (Chou et al., 1996); and anti-Rh6 rabbit 1/1000 (Tahayato et al., 2003).

Secondary antibodies were AlexaFluor488 coupled made in goat or donkey, anti-rabbit, mouse, rat or guinea pig (Molecular Probes); Cy3 or TxRed-coupled made in goat or donkey, anti-rabbit, mouse, rat, guinea pig or chicken (Jackson Immunochemicals); and Cy5 coupled made in goat or donkey, anti-mouse or rat (Jackson Immunochemicals).

Pupal retinas were staged and dissected essentially as described in Wolff (2000). They were fixed with 4% formaldehyde for 25 min and washed with PBS + 0.3% Triton X-100. Incubation with primary antibodies was performed at 4°C overnight in BNT [PBS(1×), 250 mM NaCl, 1% BSA, 1% Tween 20], and secondary antibodies (1/200 in BNT) were applied for at least 2 hr at RT.

Frozen sections of adult heads were performed as previously described (Fortini and Rubin, 1990) with antibody conditions same as above. All transgenic constructs were crossed into a *cn bw* background to eliminate eye pigmentation.

All fluorescent microscopy was performed using a Nikon Microphot-SA and super high-pressure mercury lamps (Hg 100 watts, Ushio Electric). Confocal microscopy was performed using a Leica TCS S2 system. Digital images were produced using SPOT software.

References

Bessa, J., Gebelein, B., Pichaud, F., Casares, F., and Mann, R.S. (2002). Combinatorial control of *Drosophila* eye development by *eyeless*, *homothorax*, and *teashirt*. Genes Dev. *16*, 2415–2427.

Brand, A.H., and Perrimon, N. (1993). Targeted gene expression as a means of altering cell fates and generating dominant phenotypes. Development *118*, 401–415.

Brennan, C.A., and Moses, K. (2000). Determination of *Drosophila* photoreceptors: timing is everything. Cell. Mol. Life Sci. *57*, 195–214.

Campos-Ortega, J.A., Jurgens, G., and Hofbauer, A. (1979). Cell clones and pattern formation: studies on sevenless, a mutant of Drosophila melanogaster. Wilhelm Roux's Archives *186*, 27–50.

Cavodeassi, F., Modolell, J., and Gomez-Skarmeta, J.L. (2001). The Iroquois family of genes: from body building to neural patterning. Development *128*, 2847–2855.

Chen, C.M., and Struhl, G. (1999). Wingless transduction by the Frizzled and Frizzled2 proteins of *Drosophila*. Development *126*, 5441–5452.

Chou, W.H., Hall, K.J., Wilson, D.B., Wideman, C.L., Townson, S.M., Chadwell, L.V., and Britt, S.G. (1996). Identification of a novel *Drosophila* opsin reveals specific patterning of the R7 and R8 photoreceptor cells. Neuron *17*, 1101–1115.

Chou, W.H., Huber, A., Bentrop, J., Schulz, S., Schwab, K., Chadwell, L.V., Paulsen, R., and Britt, S.G. (1999). Patterning of the R7 and R8 photoreceptor cells of *Drosophila*: evidence for induced and default cell-fate specification. Development *126*, 607–616.

Cook, T., Pichaud, F., Sonneville, R., Papatsenko, D., and Desplan, C. (2003). Distinction between color photoreceptor cell fates is controlled by Prospero in *Drosophila*. Dev. Cell *4*, 853–864.

Fortini, M.E., and Rubin, G.M. (1990). Analysis of cis-acting requirements of the Rh3 and Rh4 genes reveals a bipartite organization to rhodopsin promoters in *Drosophila melanogaster*. Genes Dev. *4*, 444–463.

Fortini, M.E., and Rubin, G.M. (1991). The optic lobe projection pattern of polarization-sensitive photoreceptor cells in *Drosophila melanogaster*. Cell Tissue Res. *265*, 185–191.

Franceschini, N., and Kirschfeld, K. (1971). In vivo optical study of photoreceptor elements in the compound eye of Drosophila. Kybernetik *8*, 1–13.

Franceschini, N., Kirschfeld, K., and Minke, B. (1981). Fluorescence of photoreceptor cells observed *in vivo*. Science *213*, 1264–1267.

Frankfort, B.J., Nolo, R., Zhang, Z., Bellen, H., and Mardon, G. (2001). *senseless* repression of *rough* is required for R8 photoreceptor differentiation in the developing *Drosophila* eye. Neuron *32*, 403–414.

Gaul, U., Mardon, G., and Rubin, G.M. (1992). A putative Ras GTPase activating protein acts as a negative regulator of signaling by the Sevenless receptor tyrosine kinase. Cell *68*, 1007–1019.

Hardie, R.C. (1984). Properties of photoreceptors R7 ansd R8 in dorsal marginal ommatidia in the compound eyes of *Musca* and *Calliphora*. J. Comp. Physiol. *154*, 157–165.

Hardie, R.C. (1985). Functional organization of the fly retina. In Progress in Sensory Physiology, H. Autrum, D. Ottoson, E.R. Perl, R.F. Schmidt, H. Shimazu, and W.D. Willis, eds. (Berlin: Springer), 1–79.

Huber, A., Schulz, S., Bentrop, J., Groell, C., Wolfrum, U., and Paulsen, R. (1997). Molecular cloning of *Drosophila* Rh6 rhodopsin: the visual pigment of a subset of R8 photoreceptor cells. FEBS Lett. *406*, 6–10.

Kauffmann, R.C., Li, S., Gallagher, P.A., Zhang, J., and Carthew, R.W. (1996). Ras1 signaling and transcriptional competence in the R7 cell of *Drosophila*. Genes Dev. *10*, 2167–2178.

Kirschfeld, K., and Franceschini, N. (1968). Optische Eigenschaften der Ommatidien im Komplexauge von *Musca*. Kybernetik *2*, 47–52.

Kirschfeld, K., and Franceschini, N. (1977). Photostable pigments within the membrane of photoreceptors and their possible role. Biophys. Struct. Mech. *3*, 191–194.

Labhart, T. (1988). Polarization-opponent interneurons in the insect visual system. Nature *331*, 435–437.

Labhart, T. (2000). Polarization-sensitive interneurons in the optic lobe of the desert ant *Cataglyphis bicolor*. Naturwissenschaften *87*, 133–136.

Labhart, T., and Meyer, E.P. (1999). Detectors for polarized skylight in insects: a survey of ommatidial specializations in the dorsal rim area of the compound eye. Microsc. Res. Tech. *47*, 368–379.

Labhart, T., and Meyer, E.P. (2002). Neural mechanisms in insect navigation: polarization compass and odometer. Curr. Opin. Neurobiol. *12*, 707–714.

McNeill, H., Yang, C.H., Brodsky, M., Ungos, J., and Simon, M.A. (1997). *mirror* encodes a novel PBX-class homeoprotein that functions in the definition of the dorsal-ventral border in the *Drosophila* eye. Genes Dev. *11*, 1073–1082.

Mlodzik, M., Hiromi, Y., Weber, U., Goodman, C.S., and Rubin, G.M. (1990). The Drosophila seven-up gene, a member of the steroid receptor gene superfamily, controls photoreceptor cell fates. Cell *60*, 211–224.

Mollereau, B., Wernet, M.F., Beaufils, P., Killian, D., Pichaud, F., Kuhnlein, R., and Desplan, C. (2000). A green fluorescent protein enhancer trap screen in *Drosophila* photoreceptor cells. Mech. Dev. *93*, 151–160.

Mollereau, B., Dominguez, M., Webel, R., Colley, N.J., Keung, B., de Celis, J.F., and Desplan, C. (2001). Two-step process for photoreceptor formation in *Drosophila*. Nature *412*, 911–913.

Moses, K., and Rubin, G.M. (1991). *Glass* encodes a site-specific DNA-binding protein that is regulated in response to positional signals in the developing *Drosophila* eye. Genes Dev. *5*, 583–593.

Moskow, J.J., Bullrich, F., Huebner, K., Daar, I.O., and Buchberg, A.M. (1995). Meis1, a PBX1-related homeobox gene involved in myeloid leukemia in BXH-2 mice. Mol. Cell. Biol. *15*, 5434–5443.

Papatsenko, D., Sheng, G., and Desplan, C. (1997). A new rhodopsin in R8 photoreceptors of *Drosophila*: evidence for coordinate expression with Rh3 in R7 cells. Development *124*, 1665–1673.

Pichaud, F., and Casares, F. (2000). *homothorax* and *iroquois-C* genes are required for the establishment of territories within the developing eye disc. Mech. Dev. *96*, 15–25.

Pichaud, F., and Desplan, C. (2001). A new visualization approach for identifying mutations that affect differentiation and organization of the *Drosophila* ommatidia. Development *128*, 815–826.

Rieckhof, G.E., Casares, F., Ryoo, H.D., Abu-Shaar, M., and Mann, R.S. (1997). Nuclear translocation of extradenticle requires *homothorax*, which encodes an extradenticle-related homeodomain protein. Cell *91*, 171–183.

Rossel, S., and Wehner, R. (1986). Polarization vision in bees. Nature *323*, 128–131.

Ryoo, H.D., Marty, T., Casares, F., Affolter, M., and Mann, R.S. (1999). Regulation of Hox target genes by a DNA bound Homothorax/Hox/extradenticle complex. Development *126*, 5137–5148.

Tahayato, A., Sonneville, R., Pichaud, F., Wernet, M.F., Papatsenko, D., Beaufils, P., Cook, T., and Desplan, C. (2003). Otd/Crx, a dual regulator for the specification of ommatidia subtypes in the *Drosophila* retina. Dev. Cell *5*, 391–402.

Tomlinson, A. (2003). Patterning the peripheral retina of the fly: decoding a gradient. Dev. Cell, in press.

Treisman, J.E., and Rubin, G.M. (1995). wingless inhibits morphogenetic furrow movement in the *Drosophila* eye disc. Development *121*, 3519–3527.

von Philipsborn, A., and Labhart, T. (1990). A behavioral study of polarization vision in the fly, *Musca domestica*. J Comp Physiol. *167*, 737–743.

Wada, S. (1974). Spezielle randzonale Ommatidien der Fliegen (Diptera: Brachycera): Architektur und Verteilung in den Komplexaugen. Z. Morph. Tiere. *77*, 87–125.

Wehner, R. (1994). The polarization-vision project: championing organismic biology. In Neural Basis of Behavioral Adaptations, K. Schildberger, N. Elsner, eds. (Stuttgart, Jena, New York; Gustav Fischer Verlag), pp. 103–143.

Wolf, R., Gebhardt, B., Gademann, R., and Heisenberg, M. (1980).

Polarization sensitivity of course control in *Drosophila melanogaster*. J. Comp. Physiol. *139*, 177–191.

Wolff, T. (2000). Histological techniques for the *Drosophila* eye part I: larva and pupa. In Drosophila Protocols, W. Sullivan, M. Ashburner, and R.S. Hawley, eds. (Cold Spring Harbor, NY: Cold Spring Harbor Laboratory Press), pp. 201–228.

Wolff, T., and Ready, D.F. (1993). Pattern formation in the *Drosophila* retina. In The Development of *Drosophila melanogaster*, M. Bate and A. Martinez-Arias, eds. (Cold Spring Harbor, NY: Cold Spring Harbor Laboratory Press), pp. 1277–1325.

Wunderer, H., and Smola, U. (1982). Fine structure of ommatidia at the dorsal eye margin of *Calliphora erythrocephala Meigen* (*Diptera, Calliphoridae*). Int. J. Insect Morphol. Embryol. *11*, 25–38.

Xu, T., and Rubin, G.M. (1993). Analysis of genetic mosaics in developing and adult *Drosophila* tissues. Development *117*, 1223–1237.

Yoshikawa, S., McKinnon, R.D., Kokel, M., and Thomas, J.B. (2003). Wnt-mediated axon guidance via the Drosophila derailed receptor. Nature *422*, 583–588.

Zuker, C.S., Cowman, A.F., and Rubin, G.M. (1985). Isolation and structure of a rhodopsin gene from *D. melanogaster*. Cell *40*, 851–858.